

Supplementary information

Preparation, characterization, and magnetic properties of poly(3-methoxythiophene)-Fe₃O₄ conducting nanocomposite

Katsuyoshi Hoshino,^{a*} Kiho Kashiwagi,^a Minako Tachiki,^a Hyuma Masu,^b and Satoru Tsukada^{a*}

^a Department of Materials Science, Graduate School of Engineering, Chiba University, 1-33 Yayoi-cho, Inage-ku, Chiba 263-8522, Japan

^b Center for Analytical Instrumentation, Chiba University, 1-33 Yayoi-cho, Inage-ku, Chiba 263-8522, Japan

Table of Contents

Elemental maps for P3MeOT-Cl	S2
EDX measurements of P3MeOT-ClO ₄ and Red 2	S3
Magnetism demonstrations for P3MeOT-ClO ₄ and Red 2	S3
XPS measurements for P3MeOT-ClO ₄	S4
XPS survey spectra of P3MeOT-Cl and Red 1	S5
EDX spectra of P3MeOT-Cl and Red 1	S5
Magnetic property measurements for Red 2	S6
Magnetic property measurements for P3MeOT-ClO ₄	S7
Supplementary References	S8

Elemental maps for P3MeOT-Cl

The results of the elemental mapping analysis of P3MeOT-Cl are shown in Fig. S1. The images exhibited minimal contrast for Fe (attributed to iron chloride) and C, O, and S (attributed to P3MeOT), suggesting a nearly uniform distribution of these elements throughout the sample. This observation corroborates the minimal contrast observed in the TEM images of P3MeOT-Cl.

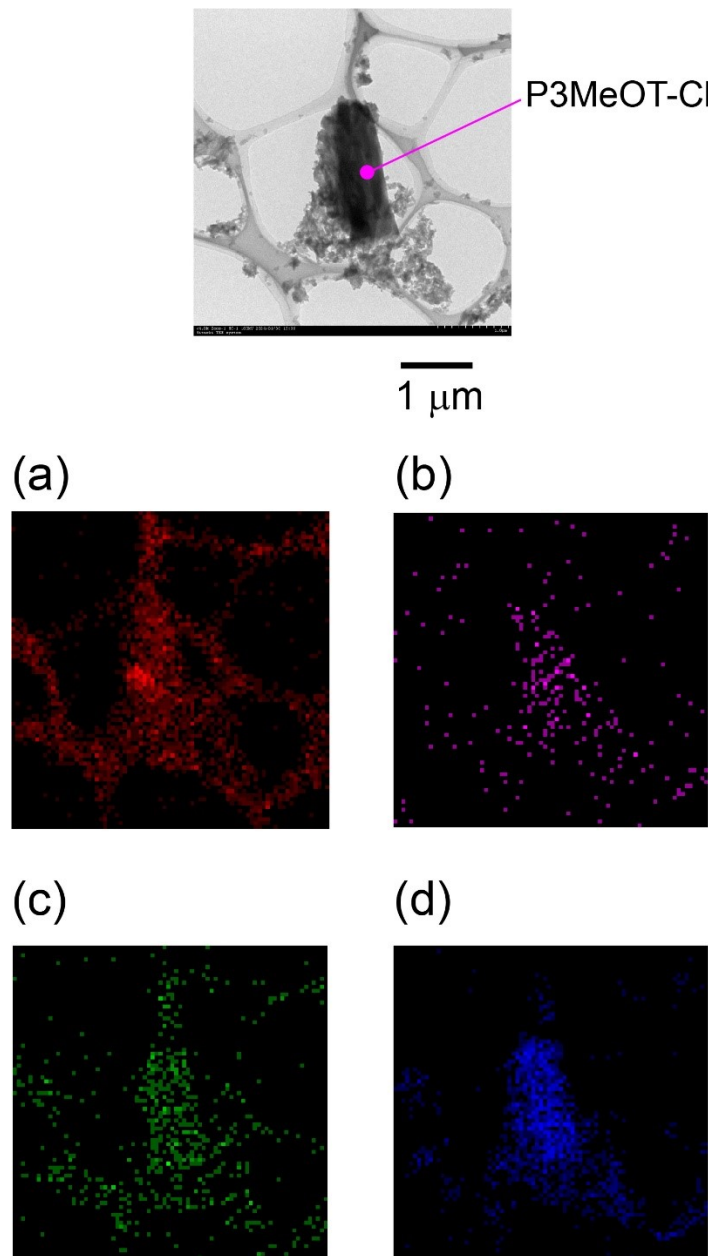


Fig. S1 EDX elemental mapping images recorded for the (a) C, (b) Fe, (c) O, and (d) S components of P3MeOT-Cl. The mapping process was conducted using the TEM image presented at the top of each elemental map.

EDX measurements of P3MeOT-ClO₄ and Red 2

The EDX elemental analysis results obtained for P3MeOT-ClO₄ and Red 2 are listed in Table S1, wherein the atomic ratios of S, Cl, and Fe are given. The atomic ratios of Cl and Fe were normalized to an atomic concentration of 1 for S. The Fe/S ratios were determined to be zero for both samples, indicating that neither P3MeOT-ClO₄ nor Red 2 contains any detectable amounts of Fe. In addition, the difference in the degree of polymerization between P3MeOT-Cl (the precursor of Red 1) and P3MeOT-ClO₄ (the precursor of Red 2) is small,¹ and so Red 2 can be regarded as a model compound that would be obtained if the Fe-containing product could be removed from Red 1.

Table S1. Atomic ratios of Cl and Fe relative to S in the P3MeOT-ClO₄ and Red 2 molecules^a

Molecule	S	Cl	Fe
P3MeOT-ClO ₄	1.00	0.27	0.00
Red 2	1.00	0.018	0.00

^a The atomic ratios were obtained by EDX measurements and normalized to S

Magnetism demonstrations for P3MeOT-ClO₄ and Red 2.

Fig. S2 shows photographic images of the P3MeOT-ClO₄ and Red 2 powders being brought close to a ferrite magnet through a glass vial. Since neither P3MeOT-ClO₄ nor Red 2 is attracted to the black circular magnet placed at the center of the blue plastic support, it can be concluded that they do not exhibit strong magnetism.

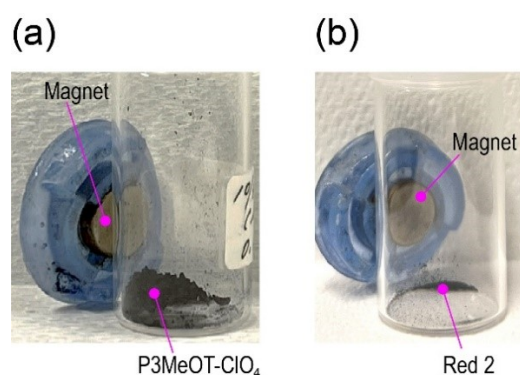


Fig. S2 Photographic images showing the behaviors of the (a) P3MeOT-ClO₄ and (b) Red 2 powders when brought close to a magnet. The diameter of the glass vial is 20 mm.

XPS measurements for P3MeOT-ClO₄

Fig. S3 shows the XPS spectra recorded for the Fe 2p_{3/2}, O 1s, and Cl 2p components of P3MeOT-ClO₄. In the Fe 2p_{3/2} spectrum, no signal is observed, indicating that Fe originating from the oxidizing agent, Fe(ClO₄)₃, is not present in the P3MeOT-ClO₄ structure. Additionally, the O 1s spectrum shows a peak centered at 531.7 eV, which was attributed to superposition of the signals originating from the methoxy oxygen moiety of P3MeOT and the ClO₄⁻ dopant. In the Cl 2p spectrum, two peaks can be observed at 205.6 and 207.1 eV, which were attributed to the Cl 2p_{3/2} and Cl 2p_{1/2} components of Cl in ClO₄⁻. Compared with the values observed for Cl⁻ (see Fig. 6 in the main text), these values are shifted toward higher binding energies. This shift was caused by a partial displacement of the chlorine valence electrons in ClO₄⁻ toward the oxygen atoms. Consequently, this displacement strengthens the interactions between the Cl 2p electrons and the chlorine nucleus.

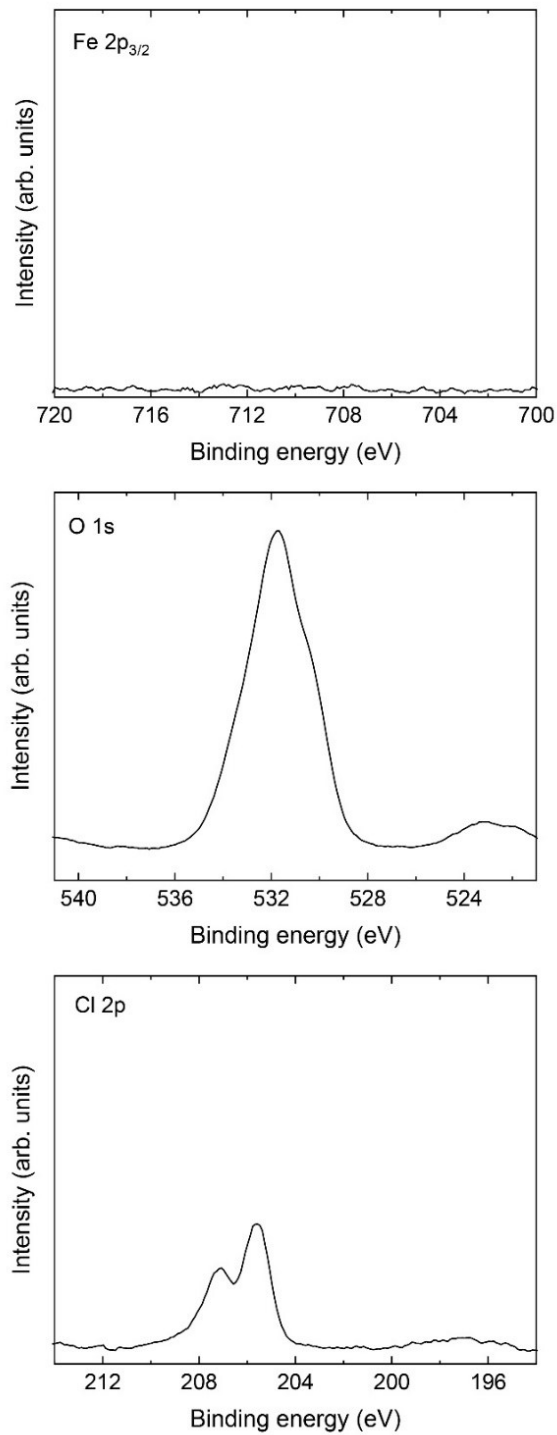


Fig. S3 XPS spectra of the Fe 2p_{3/2} (top), O1s (middle), and Cl 2p (bottom) components of P3MeOT-ClO₄.

As a result, the binding energy of the Cl 2p electrons increases, leading to the observed shift in binding energy shown in Fig. S3.²

XPS survey spectra of P3MeOT-Cl and Red 1

Fig. S4 shows the XPS survey spectra recorded for P3MeOT-Cl and Red 1. As can be seen, no detectable amount of nitrogen was observed in the N 1s binding energy region around 400 eV, indicating that neither P3MeOT-Cl nor Red 1 contain nitrogen.

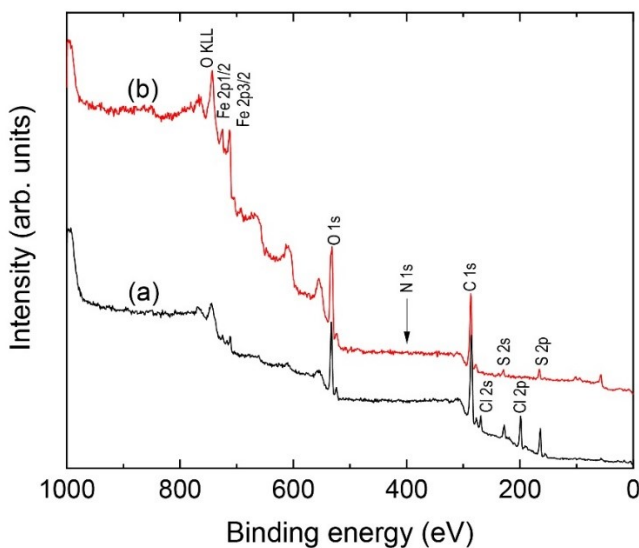


Fig. S4 XPS survey spectra recorded for (a) P3MeOT-Cl and (b) Red 1.

EDX spectra of P3MeOT-Cl and Red 1

Fig. S5 shows the EDX spectra recorded for P3MeOT-Cl and Red 1, in addition to their corresponding SEM images. In the EDX spectra, if N were present, its N $\text{K}\alpha$ signal would be expected to appear at 0.39 keV, namely between the carbon (C $\text{K}\alpha$: 0.28 keV) and oxygen (O $\text{K}\alpha$: 0.53 keV) peaks.^{3,4} However, since no signal corresponding to N was detected in either of the spectra, it was deduced that neither P3MeOT-Cl nor Red 1 contains nitrogen. This finding supports the results shown in Fig. S4.

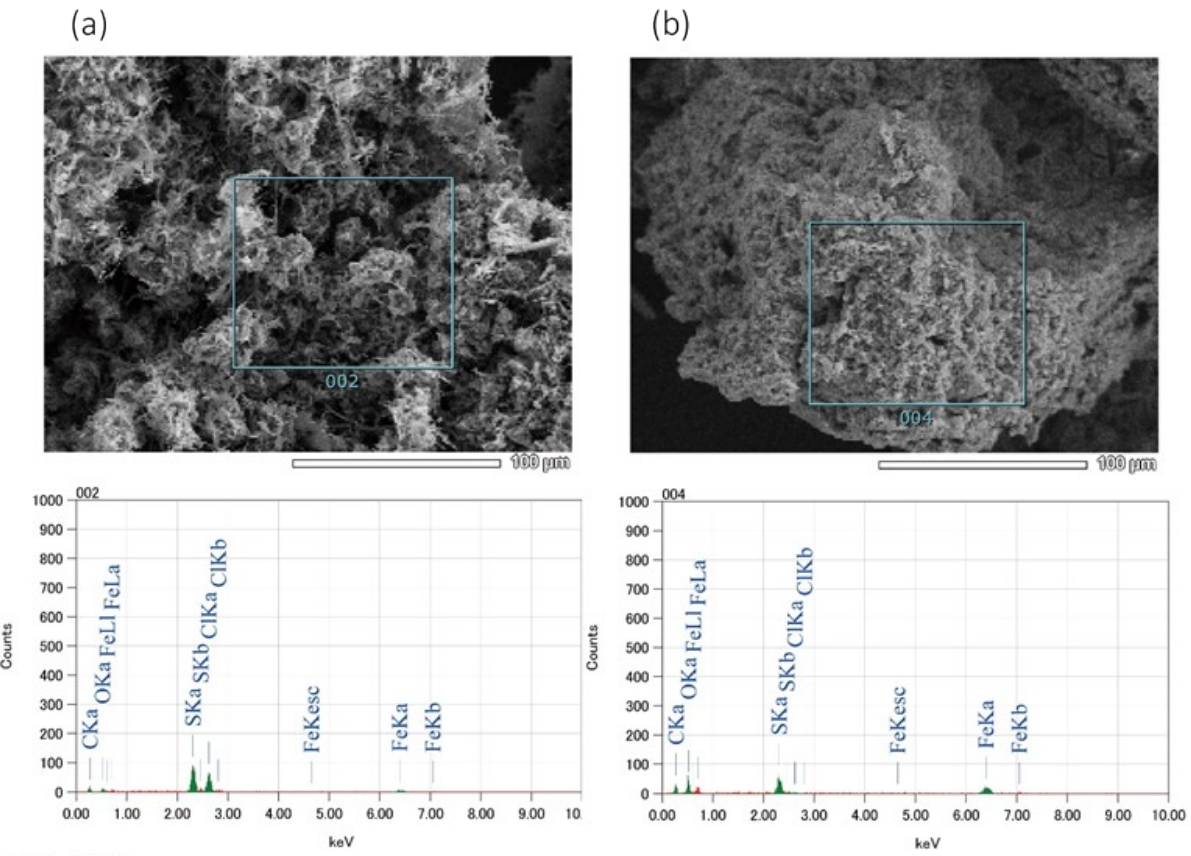


Fig. S5 EDX spectra recorded for (a) P3MeOT-Cl and (b) Red 1. Above each spectrum, the corresponding SEM image is presented.

Magnetic property measurements for Red 2

Fig. S6 shows the magnetic hysteresis loop of Red 2 measured at 5 K and its magnified view along the y-axis. The magnified hysteresis loop exhibits a saturation magnetization of 0.1 emu/g under a 50 kOe magnetic field, which is negligibly small compared to that of Red 1 (i.e., 20.2 emu/g under a 50 kOe magnetic field; see subsection 3.8 of the main text). A similar trend was observed at 300 K. Consequently, it was apparent that the development of magnetization in Red 1 is not attributable to the P3MeOT backbone, but rather to Fe_3O_4 .

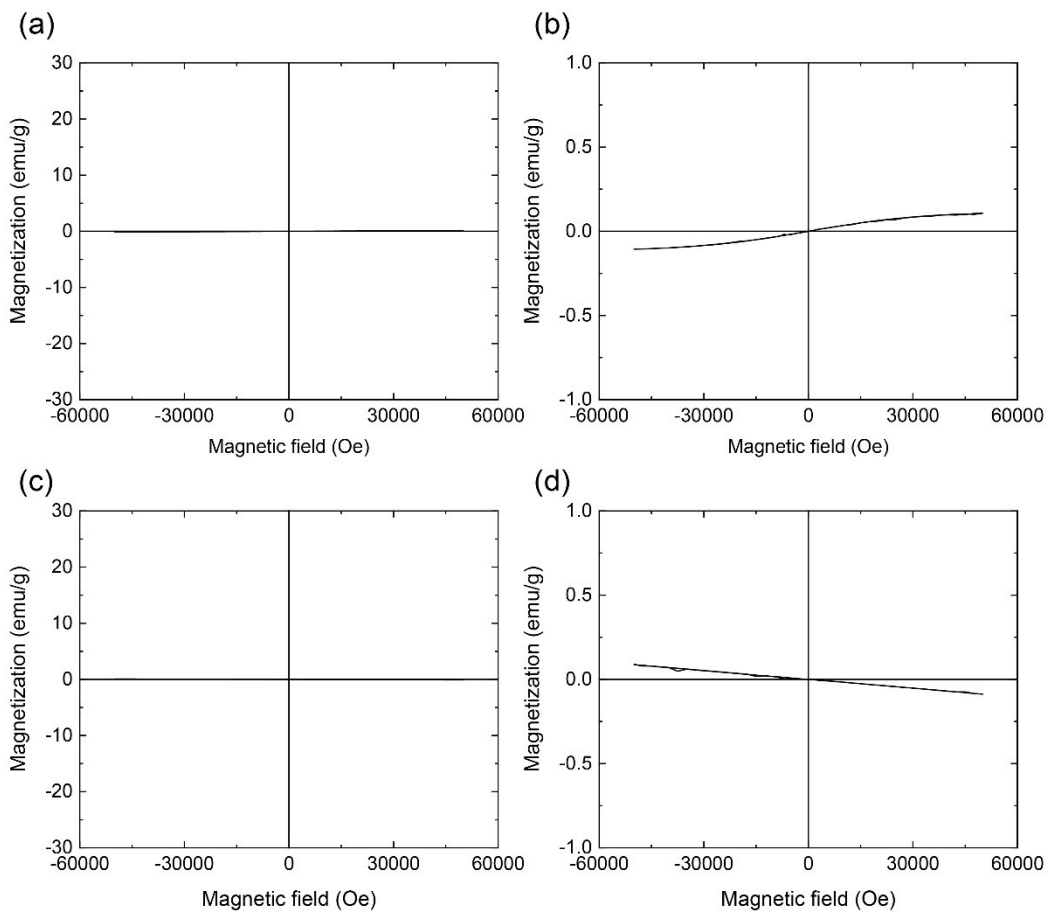


Fig. S6 Magnetic hysteresis loops of Red 2 recorded at (a, b) 5 K and (c, d) 300 K. Panels (b) and (d) represent expanded views of the data presented in panels (a) and (c), respectively.

Magnetic property measurements for P3MeOT-ClO₄

Fig. S7 shows the magnetic hysteresis loop of P3MeOT-ClO₄ measured at 5 K and its magnified view along the y-axis. The magnified hysteresis loop exhibits a saturation magnetization of 0.2 emu/g under a 50 kOe magnetic field, which is negligibly small compared to that of Red 1 (i.e., 20.2 emu/g under a 50 kOe magnetic field; see subsection 3.8 of the main text). A similar trend was observed at 300 K.

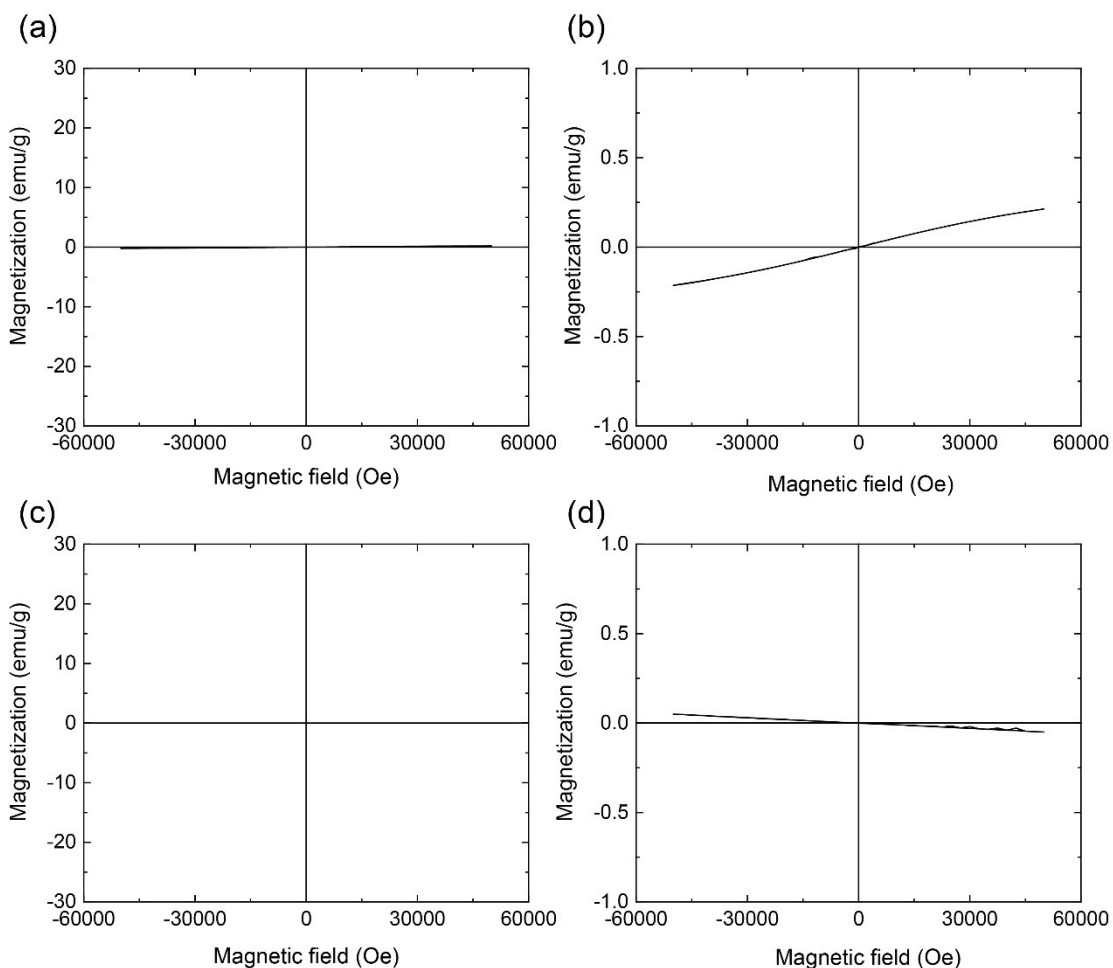


Fig. S7 Magnetic hysteresis loops of P3MeOT-ClO₄ recorded at (a, b) 5 K and (c, d) 300 K. Panels (b) and (d) represent expanded views of the data presented in panels (a) and (c), respectively.

Supplementary References

- 1 Supporting Information in: M. Tachiki, R. Tagawa and K. Hoshino, Oligo(3-methoxythiophene)s as Water-Soluble Dyes for Highly Lustrous Gold- and Bronze-Like Metal-Effect Coatings and Paintings, *ACS Omega*, 2020, **5**, 24379–24388.
- 2 Y. Zhang, S. Mu, B. Deng, J. Zheng, Electrochemical Removal and Release of Perchlorate Using Poly(aniline-co-o-aminophenol), *J. Electroanal. Chem.*, 2010, **641**, 1–6.
- 3 Y. Ye, J. Chen, Q. Ding, D. Lin, R. Dong, L. Yang, J. Liu, Sea-Urchin-Like Fe₃O₄@C@Ag Particles: an Efficient SERS Substrate for Detection of Organic Pollutants, *Nanoscale*, 2013, **5**, 5887–5895.
- 4 D. Menga, F. Ruiz-Zepeda, L. Moriau, M. Šala, F. Wagner, B. Koyutürk, M. Bele, U. Petek, N. Hodnik, M. Gaberšček, T.-P. Fellinger, *Adv. Energy Mater.*, 2019, **9**, 1902412.